Chapter 4

Results, Analysis and Discussions (Part I): Silicon Carbide Thin Films from RF-PECVD, DC-PECVD and HW-CVD Techniques

4.1 Introduction

This chapter discusses the results obtained from the characterization of silicon carbide thin films prepared by using three deposition techniques. The deposition techniques that were discussed in this part are Radio Frequency Plasma Enhanced Chemical Deposition (RF-PECVD), Direct Current Plasma Enhanced Chemical Deposition (DC-PECVD) and Hot-Wire Chemical Deposition (HW-CVD). The effects of methane to silane gas flow rate ratio on the optical and structural properties of the films were studied. For each technique, analysis of results from the Optical Transmission spectroscopy is first presented, followed by the Fourier Transformed Infrared spectroscopy, Micro-Raman spectroscopy and X-Ray Diffraction spectroscopy. From the optical transmission spectra, the effects of methane to silane gas flow rate ratio on the deposition rate and optical energy gap are depicted and discussed. Discussions on the microstructures of the films are presented in the next section in sequence to the presentation of the results obtained from the FTIR spectroscopy. Here, the results from FTIR measurements are first detailed, followed by analysis on the effects of methane to silane gas flow rate ratio on the Si-C and Si-H bonding configuration in the films. Finally, this is followed by presentation and discussions on the results obtained from Micro-Raman and XRD measurements which were performed to assist the study on the film structure of the silicon carbide thin films produced in this work.

4.2 Optical Transmission Spectra of Silicon Carbide Thin Films Prepared at Different Methane to Silane Gas Flow Rate Ratio

Optical transmission spectra of silicon carbide thin films prepared by RF-PECVD, DC-PECVD and HW-CVD techniques at different methane to silane gas flow rate ratio are shown in Figure 4.1(a), Figure 4.1(b) and figure 4.1(c) respectively. As

can be seen from the figures, the silicon carbide thin films prepared using these techniques were affected by methane to silane gas flow rate ratio. Generally, lower methane to silane gas flow rate ratio produces silicon carbide thin films that absorb UV light at higher wavelength in the range of 450 nm to 550 nm. Silicon carbide thin films prepared by DC-PECVD display the largest variation in absorption which decreases in wavelength as the gas flow rate ratio increases.

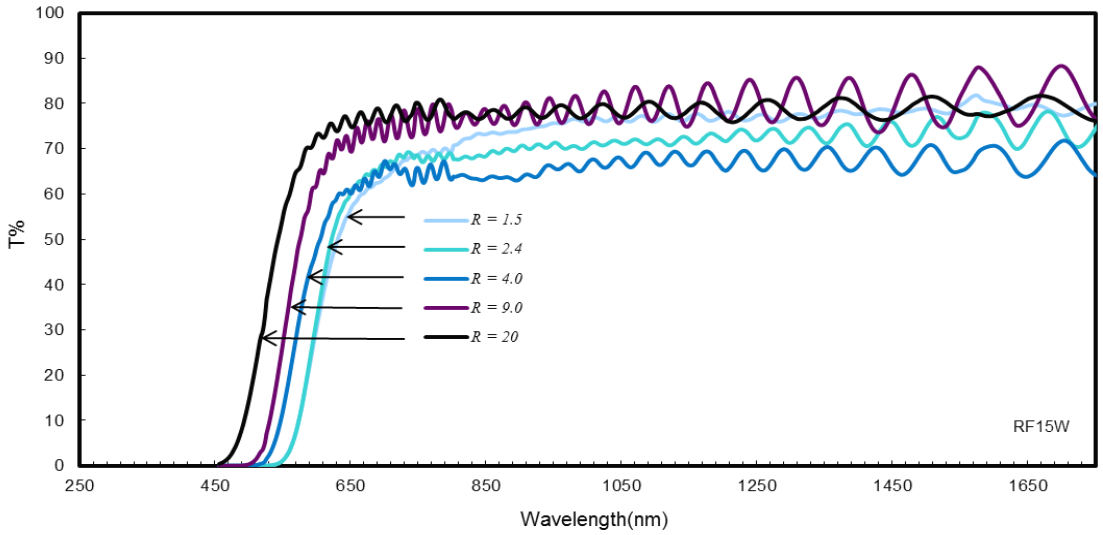

Figure 4.1(a): Optical transmission spectra of SiC thin films prepared at different methane to silane gas flow rate ratio by RF-PECVD technique.

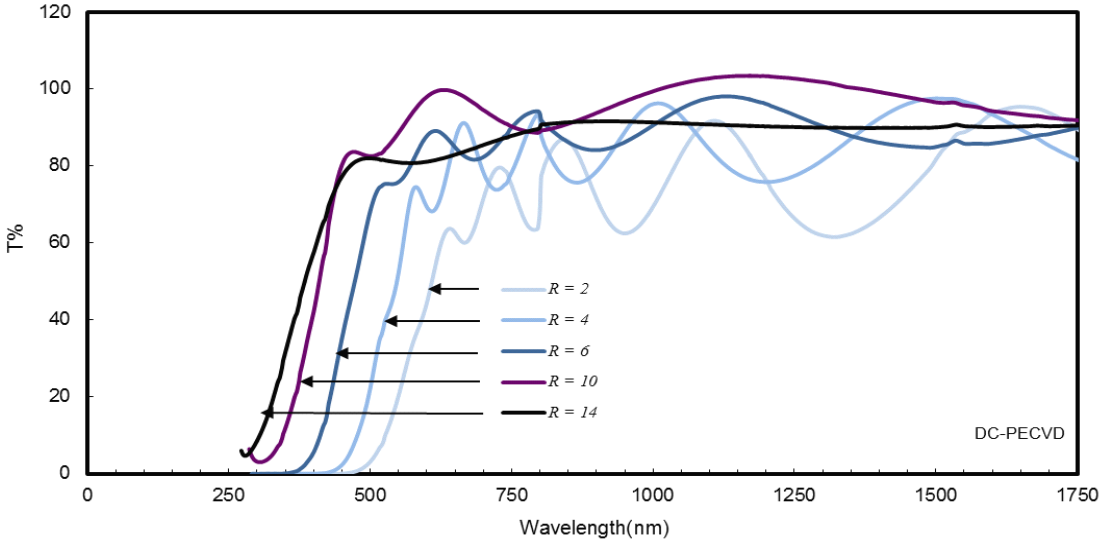

Figure 4.1(b): Optical transmission spectra of SiC thin films prepared at different methane to silane gas flow rate ratio by DC-PECVD technique.

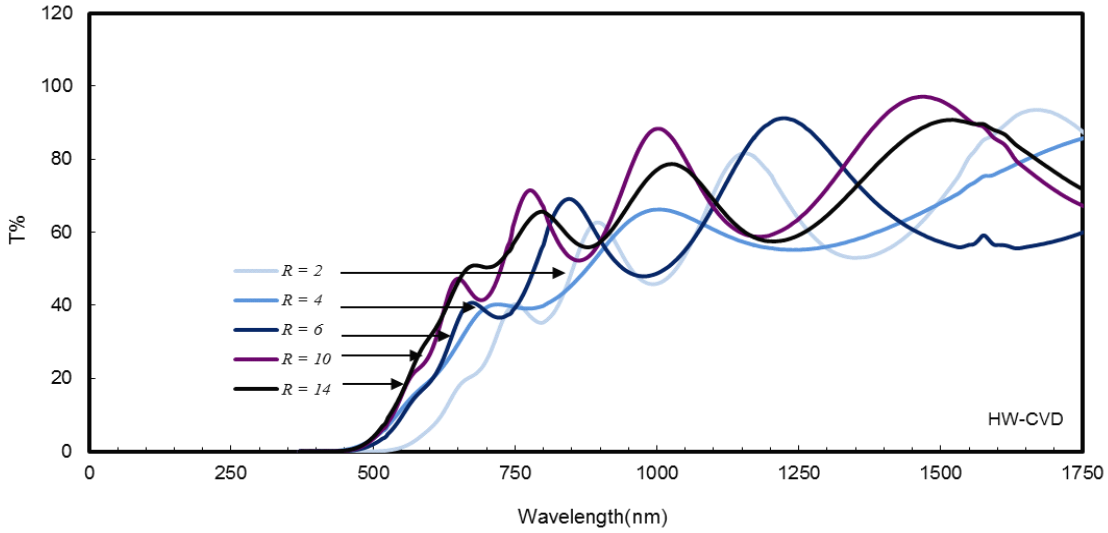

Figure 4.1(c): Optical transmission spectra of SiC thin films prepared at different methane to silane gas flow rate ratio by HW-CVD technique.

4.2.1 The Effects of Methane to Silane Gas Flow Rate Ratio on the Deposition Rate of Silicon Carbide Thin Films

The deposition rate of the silicon carbide thin films prepared by various techniques as a function of *R* is shown in Figure 4.2. The deposition rates of the silicon carbide thin films prepared by DC-PECVD technique which varies between 0.05 nm/s and 0.25 nm/s is obviously the lowest deposition rate as compared to the other two techniques. The deposition rate for RF-PECVD thin films varies between 2.25 nm/s and 1.00 nm/s while for HW-CVD thin films the deposition rate varies from 0.5 to 2.0 nm/s.

The deposition rate of the RF-PECVD films decreases with increase in *R*. The DC-PECVD films shows no significant change with increase in *R* up to *R*=10 but films prepared at *R*=14 shows a slight increase in deposition rate. These differences in deposition rate and variation in deposition rate over *R* reflects that the deposition kinetics in relation to *R* is different for every different deposition technique.

Secondary gas phase reaction produces growth radicals as well as reactive hydrogen atoms. The decrease in deposition rate with increase in *R* for the film deposited by RF-PECVD shows that hydrogen etching effect increases with increase in

R. This result also indicates that the number of hydrogen atoms that reaches the growth surface exceeds the number of growth radicals and it (the number of hydrogen atoms) increases in dominance by the increase in methane to silane gas flow rate ratio.

For DC-PECVD films, the dissociation rate is low and the number of growth radicals and hydrogen atoms reaching the growth sites are also low; thus increase in *R* has no significant effect on the deposition rate. The slight increase in deposition rate for the film prepared at the highest *R* of 14 as seen in Figure 4.2 shows that at this methane to silane gas flow rate ratio, the number of growth radicals reaching the substrate is more dominant as compared to the reactive hydrogen atoms. At *R*=14, although dissociation rate is low, the high concentration of methane gas molecules has resulted in increased number of hydrogen atom which has effectively created growth sites for the growth radicals. The more dominant presence of growth radicals in the deposition chamber, due to the slow dissociation process, has in turn resulted in increased deposition rate (*R*=14).

The HW-CVD deposition mechanism clearly shows a different deposition mechanism from the other two deposition techniques. The deposition rate is high at the lowest *R* and decreases to a low value for films prepared at *R*=4. Further increase in *R* resulted in an increase in deposition rate. In HW-CVD, growth radicals are produced from the dissociation of the precursor gas molecules; both silane and methane, but they are produced at relatively higher dissociation rate from silane. At very low *R* (*R*=2), the pumping rate was decreased to maintain the pressure within the reaction chamber. This has allowed longer mean free path for the growth radicals. These energetic growth radicals reach the growth site at high intensity and create its own growth sites by abstraction process, which is, breaking passivated bonds at the growth surface and thus resulted in high film deposition rate. However, at *R*=4, a rapid decrease in deposition

rate is noted as in Figure 4.2. Increase in methane to silane gas flow rate ratio to R=4 has further increases the number of methane molecules in the reaction chamber. This increases the number of hydrogen atoms reaching the growth surface thus increases the hydrogen etching effects. Consequently, growth sites are created but the less dominance of growth radicals present at this growth sites has allowed the hydrogen atoms to be passivating the dangling bonds hence resulted in low film deposition rate. Further increase in the methane to silane gas flow rate ratio (R>4) in the reaction chamber resulted in increase in secondary gas phase reactions through collisions with methane molecules. These reactions deplete the number of hydrogen atoms but increase the number of growth radicals reaching the growth sites. Therefore for R>4, deposition rate increases. This does not happen in the RF-PECVD process because in RF-PECVD, hydrogen atoms are produced in larger number even during the primary dissociation of precursor gases as both silane and methane molecules are actively dissociated. Therefore it is confirmed that in HW-CVD, the hot tungsten filament is more active in dissociation of silane gas and dissociation of methane is comparatively very low.

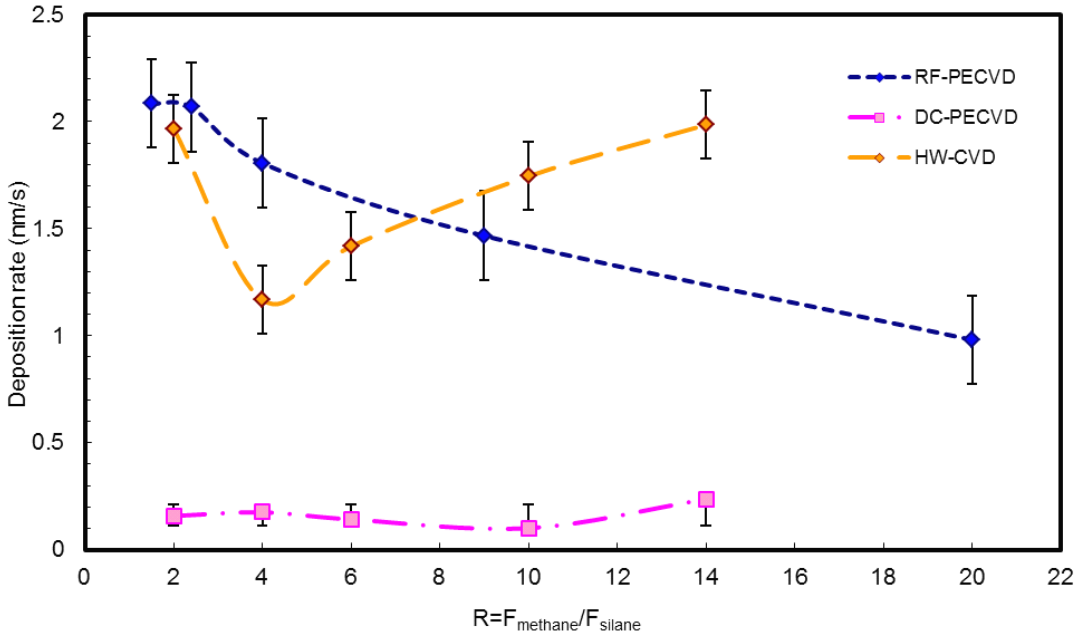

Figure 4.2: Deposition rate of SiC thin films prepared at various methane to silane gas flow rate ratio by RF-PECVD, DC-PECVD and HW-CVD techniques.

4.2.2 The Effects of Methane to Silane Gas Flow Rate Ratio on the Optical Energy Gap of Silicon Carbide Thin Films

Generally, the silicon carbide films prepared by DC-PECVD has the largest values of optical energy gap as compared to the silicon carbide thin films prepared by RF-PECVD and HW-CVD especially for *R* values larger than 4.

Figure 4.3 shows the dependence of optical band gap of silicon carbide films on *R* for the films prepared by RF-PECVD, DC-PECVD and HW-CVD techniques. Generally, the optical band gap of these films increases with increase in *R*. This has also been observed by other researchers in related experiment (Wang *et al.,* 1999, Tabata *et al.,* 2004, Chang and Sakai, 2004, King *et al.,* 2011). The optical band gap for the films prepared by RF-PECVD increase from 1.92 eV to 2.20 eV with increase in *R* from 1.5 to 20. The DC-PECVD technique shows a more effective band gap variation with increase in *R* compared to the other two techniques with band gap varying from 1.97 eV to 2.52 eV as *R* increases from *R*=2 to *R*=14. Similar to the trend showed by silicon carbide films prepared by RF-PECVD and DC-PECVD, the silicon carbide films

prepared by HW-CVD also show that higher methane to silane gas flow rate ratio has resulted in higher optical energy gap. However, the films prepared by HW-CVD technique shows the smallest variation of optical band gap from 1.63 eV to 1.85 eV with the values being the lowest compared to the other two techniques. The low optical energy band gap for the HW-CVD films may be contributed by increase in carbon content in the film structure. Xu *et al.* (2005) reported that increase in carbon content in SiC thin films resulted in the formation of methyl configurations thus increasing the number of micro voids and defect states in the film. If this is true, the film deposited by RF-PECVD and DC-PECVD techniques has lower carbon incorporation. The low deposition rate of the DC-PECVD films may also result in a more ordered film structure. In other words, for films prepared by these techniques, although the ratio of methane to silane gas flow was increased, carbon incorporation was kept to a minimum thus minimizing also the formation of micro voids and defect states which kept the optical energy gap at relatively large values. The blue shift which were clearly seen in the optical transmission spectra for these films as in Figure 4.1(a) and Figure 4.1(b) was in conjunction to the increasingly ordered structure of the films as the above mentioned. Film thickness is not a matter of discussion because it was reflected by the deposition rate. In this work, it was found that the deposition rate and the optical energy band gap were not affected by the gas flow rate ratio in the same manner therefore the blue shift was not in conjunction to the film thickness.

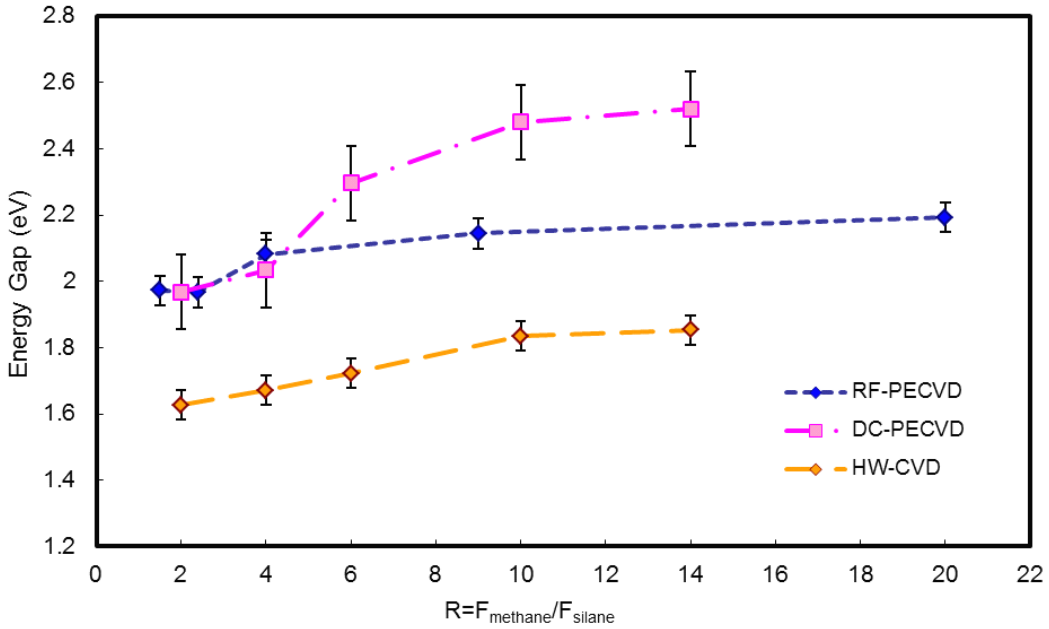

Figure 4.3: Optical energy gap of SiC thin films prepared at different methane to silane gas flow rate ratio by RF-PECVD, DC-PECVD and HW-CVD techniques.

The values obtained from the HW-CVD technique is 70-80% lower as compared to the other techniques. The value of the optical energy gap obtained by HW-CVD is only 1.63 eV for R=2 and increases to 1.85 eV for R=14. The small values of optical energy gap for the silicon carbide films prepared by HW-CVD may be related to the molecular structures and composition of the films. This will be discussed in conjunction with the bonding configurations in the next sub-section.

4.3 Fourier Transformed Infrared Spectra of Silicon Carbide Thin Films Prepared at Different Methane to Silane Gas Flow Rate Ratio

The FTIR spectra in the wavenumber region of 400 cm^{-1} to 4000 cm^{-1} for the silicon carbide thin films prepared by RF-PECVD, DC-PECVD and HW-CVD techniques is shown is Figure 4.4(a), Figure 4.4(b) and Figure 4.4(c) respectively. These figures show the vibration modes in the range of 500-1500 cm^{-1} which show entities such as Si-H wagging mode at 650 cm^{-1} (Tabata *et al.,* 2004 and Kumbhar *et al.,* 2001), combination of Si-C stretching mode at 790 cm^{-1} (Kaneko *et al.*, 2005) and Si-$(CH_3)_n$

wagging mode at 780 cm^{-1} (Tabata *et al.,* 2004) and C-H_2 bending mode at 1030 cm^{-1}. The entity of Si-H_n stretching mode at 2100 cm^{-1} is also shown clearly in these figures.

The infrared analysis are concentrated in the region between 400 cm^{-1} to 1300 cm^{-1}, 1200 cm^{-1} to 1800 cm^{-1} and 1800 cm^{-1} to 2300 cm^{-1}. The region between 400 cm^{-1} to 1300 cm^{-1} consisted of Si-H wagging band at 650 cm^{-1}, combination of Si-C stretching band at 790 cm^{-1} and Si-$(CH_3)_n$ wagging band at 780 cm^{-1} and C-H_2 bending band at 1030 cm^{-1}. The films prepared by RF-PECVD showed significant presence of Si-H_n wagging, Si-C stretching and C-H_2 bending bands as could be seen in Figure 4.4(a). The presence of interference fringes in longer wavenumber region indicates that these films are very thick and this has contributed to the higher intensity of these vibrational bands. These bands are also observed in the FTIR spectra of the films prepared by DC-PECVD but with lower intensity and that for obvious reason these films are thinner. The silicon carbide absorption bands decreases in intensity with increase in *R* but Si-H_2 wagging and C-H_2 bending bands appear to increase in intensity with increase in *R*. This is attributed to the increase in hydrogen concentration in the film with increase in *R* as explained earlier in the deposition mechanism (Sub-section 4.2.1) that the probability of reactive hydrogen atoms reaching the growth sites is higher with increase in methane gas flow rate. This was seen earlier to reduce the deposition rate of the films.

The Si-C stretching band is most dominant in the silicon carbide films prepared by HW-CVD such that the Si-H wagging and C-H_2 bending bands are almost un-significant. In the wavenumber region between 1200 cm^{-1} and 1800 cm^{-1} some unclear signals are produced but two consistent vibration peaks are observed at 1250 cm^{-1} and 1530 cm^{-1} representing Si-CH_2 and Si-CH_3 bending modes respectively and are believed to be asymmetric mode deformation (Das, Chattopadhyay and Barua, 1998). These

peaks are overlapped with the interference fringes in the infrared spectra of the RF-PECVD films. These peaks are observed in both the infrared spectra for PECVD films but were not significant in the HW-CVD films. The Si-H_n stretching bands of these films show significant presence in the infrared spectra of the RF-PECVD films prepared at all values of *R*. The decreasing pattern of intensity for this absorption is similar to the absorption band observed in the films prepared at high *R* (*R*≥6) for both the DC-PECVD and HW-CVD films. These results confirm earlier indication from the deposition rate analysis that the presence of reactive hydrogen atoms at the growth surface is very dominant for the PECVD prepared films. This contributes to the decrease in deposition rate with increase in *R*. The presence of hydrogen atoms at the growth sites only became significant at high *R* of 6 or higher for the HW-CVD. This shows that to increase the presence of reactive hydrogen atoms at the growth surface, the methane gas flow rate must be high especially for deposition by techniques where dissociation rate of methane is low.

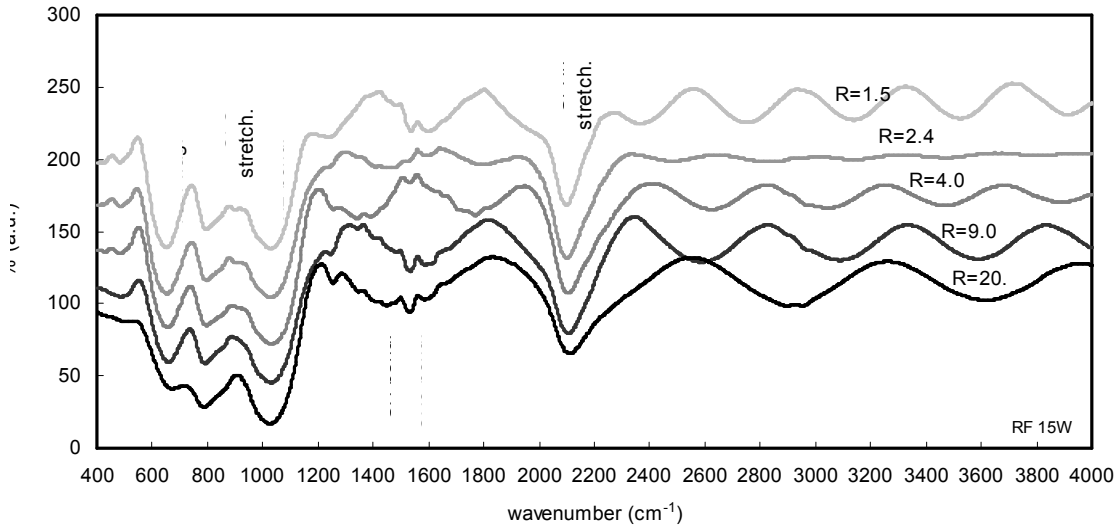

Figure 4.4(a): Fourier Transformed Infrared spectra of SiC thin films prepared at different methane to silane gas flow rate ratio by RF-PECVD technique.

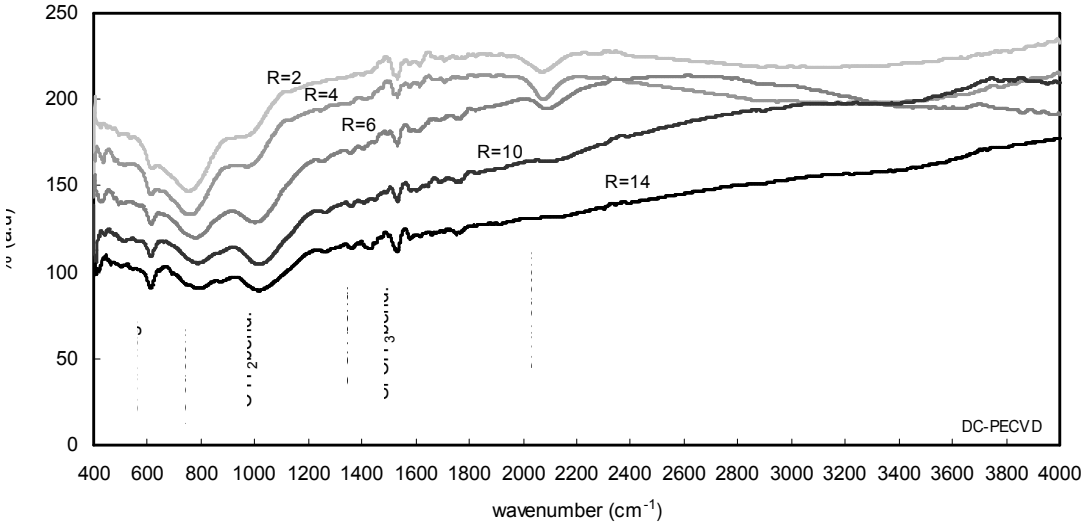

Figure 4.4(b): Fourier Transformed Infrared spectra of SiC thin films prepared at different methane to silane gas flow rate ratio by DC-PECVD technique.

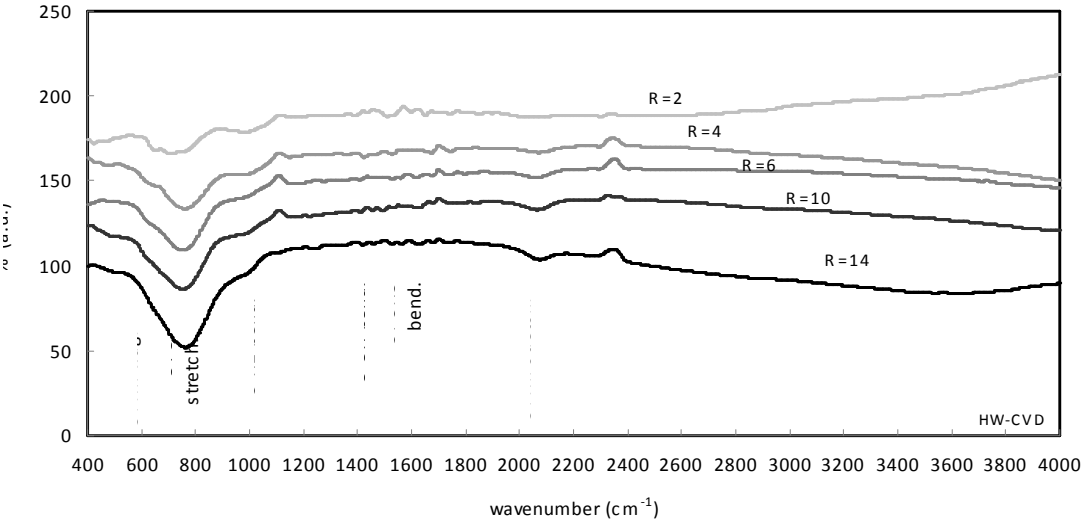

Figure 4.4(c): Fourier Transformed Infrared spectra of SiC thin films prepared at different methane to silane gas flow rate ratio by HW-CVD technique.

Figure 4.4(a) shows the FTIR spectra for silicon carbide films prepared at various methane to silane gas flow rate ratios (*R*) by RF-PECVD technique. All the films show clear entities of Si-H wagging mode at 650 cm^{-1} (Tabata *et al.,* 2004, Kumbhar *et al.,* 2001), combination of Si-C stretching mode at 790 cm^{-1} (Kaneko *et al.,* 2005) and Si-$(CH_3)_n$ wagging mode at 780 cm^{-1} (Tabata *et al.,* 2004), C-H_2 bending mode at 1030 cm^{-1} and Si-H_n stretching mode at 2100 cm^{-1}.

Figure 4.4(b) shows the FTIR spectra for the silicon carbide thin films prepared by DC-PECVD technique. The same entities are observed using DC-PECVD as those found in silicon carbide films prepared using RF-PECVD system. Si-H_n wagging mode at 650 cm^{-1}, combination of Si-C stretching mode and Si-$(CH_3)_n$ wagging mode at 780 cm^{-1}, and C-H_2 bending mode at 1030 cm^{-1} are identified in the films. However, the silicon carbide films prepared by DC-PECVD show smaller vibration band at 780 cm^{-1} which belongs to Si-C stretching mode. A shift is also observed for this band towards higher wave number (780 cm^{-1} to 800 cm^{-1}) as *R* increases. Si-H_n stretching mode which is identified at 2100 cm^{-1} is present clearly only for films prepared at low *R* (*R*=2,4,6) but appear to be very weak for films prepared at high *R* (*R*=10,14). Other significant peaks are observed at 1365 cm^{-1}, 1430 cm^{-1} and 1535 cm^{-1}. Vibration peak at 1430 cm^{-1} is believed to be the identity of the bending mode for C-CH bond and vibration peak at 1535 cm^{-1} is reported to be the identity of Si-CH_3 bending mode (Das, Chattopadhyay and Barua, 1998). These vibration peaks are especially clear for films prepared at high *R* (*R*=10,14). It is also observed that for films prepared at higher *R*, a decrease in Si-H stretching mode (2100 cm^{-1}) is parallel to an increase in the Si-H wagging mode (650 cm^{-1}). In contradiction, a slight increase in Si-CH_3 bending mode (1535 cm^{-1}) is followed by a decrease in a combination of Si-CH_3 wagging mode and Si-C stretching mode at the same vibration peak (780 cm^{-1}).

The FTIR spectra for the silicon carbide thin films prepared by HW-CVD show a constant revolution of absorption bands as shown in Figure 4.4(c). A broad peak is observed in the wave number region between 400 cm^{-1} and 1300 cm^{-1} which consist of Si-H_n wagging mode at 650 cm^{-1}, combination of Si-C stretching mode and Si-$(CH_3)_n$ wagging mode at 790 cm^{-1}, and C-H_2 bending mode at 1030 cm^{-1}. Generally, the intensity of this peak increases as *R* increase but for silicon carbide films prepared at

lower *R*, the existence of these three identities are more distinguished. The vibration of Si-H_n stretching mode is observed at 2050 cm^{-1} in all films and its intensity increases as *R* increase.

Some unclear signals are observed in the wave number region between 1200 cm^{-1} and 1800 cm^{-1}, but there is no significant peak within this range for the silicon carbide films prepared by HW-CVD technique, as that observed in the FTIR spectra for the silicon carbide films prepared by RF-PECVD and DC-PECVD techniques. Besides that, neither the signature of C-H_2 at 2890 cm^{-1} nor C-H_3 at 2960 cm^{-1} is present in the silicon carbide films prepared by HW-CVD technique.

4.3.1 The Effects of Gas Flow Rate Ratio on the Si-C and Si-H Bonding Configurations

Figure 4.5 and Figure 4.6 shows the absorption coefficient of vibration modes in 500-1500 cm^{-1} wavenumber region and absorption coefficient of Si-H_n stretching mode at approximately 2050 cm^{-1} respectively of SiC thin films prepared at different methane to silane gas flow rate ratio by RF-PECVD, DC-PECVD and HW-CVD techniques. Integrated intensity of Si-C bands as compared to the Si-H_n bands for the SiC films are shown in Figure 4.7.

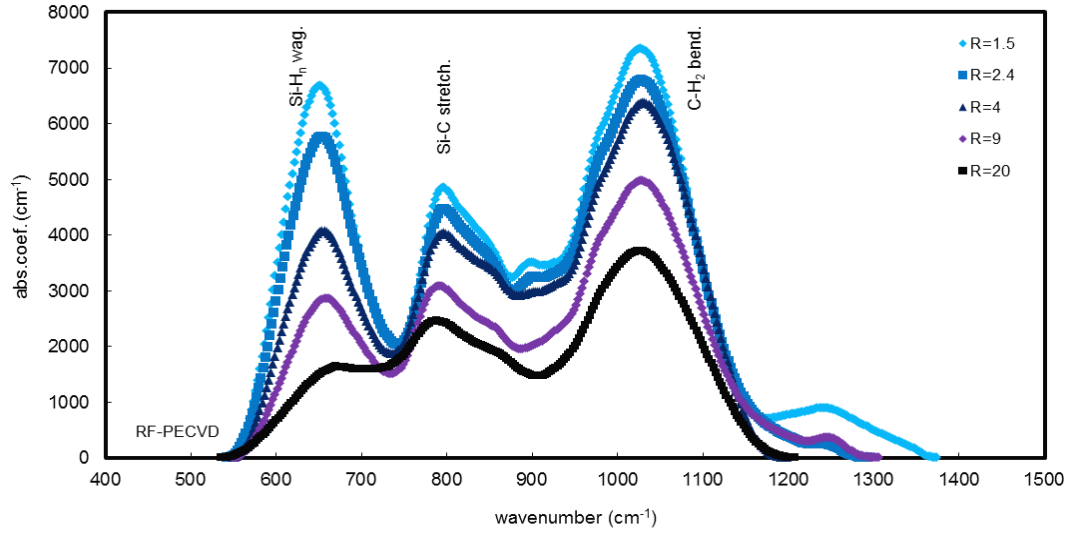

Figure 4.5(a): Absorption coefficient of vibration modes in 500-1500 cm^{-1} wavenumber region of SiC thin films prepared at different methane to silane gas flow rate ratio by RF-PECVD technique.

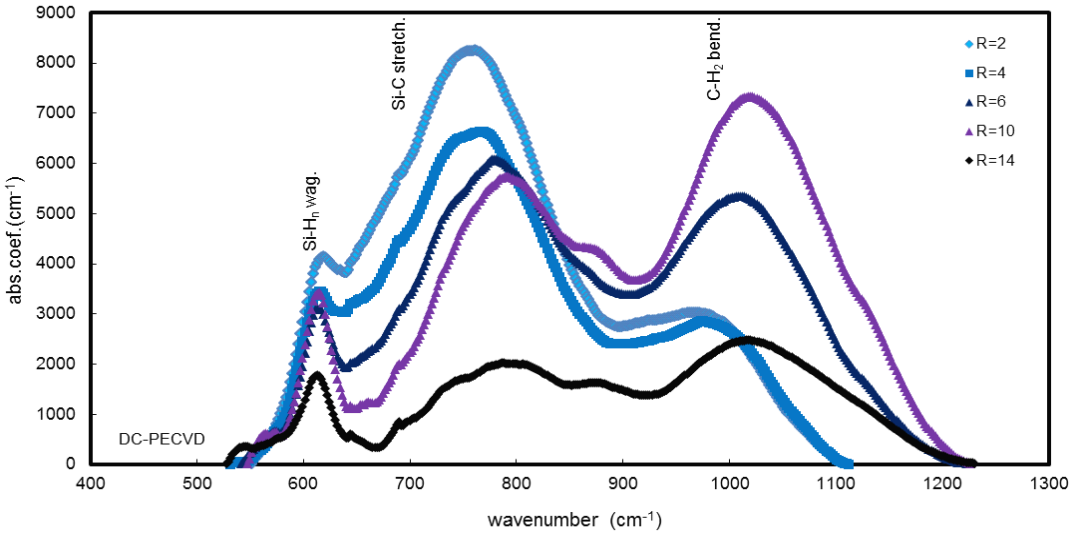

Figure 4.5(b): Absorption coefficient of vibration modes in 500-1500 cm^{-1} wavenumber region of SiC thin films prepared at different methane to silane gas flow rate ratio by DC-PECVD technique.

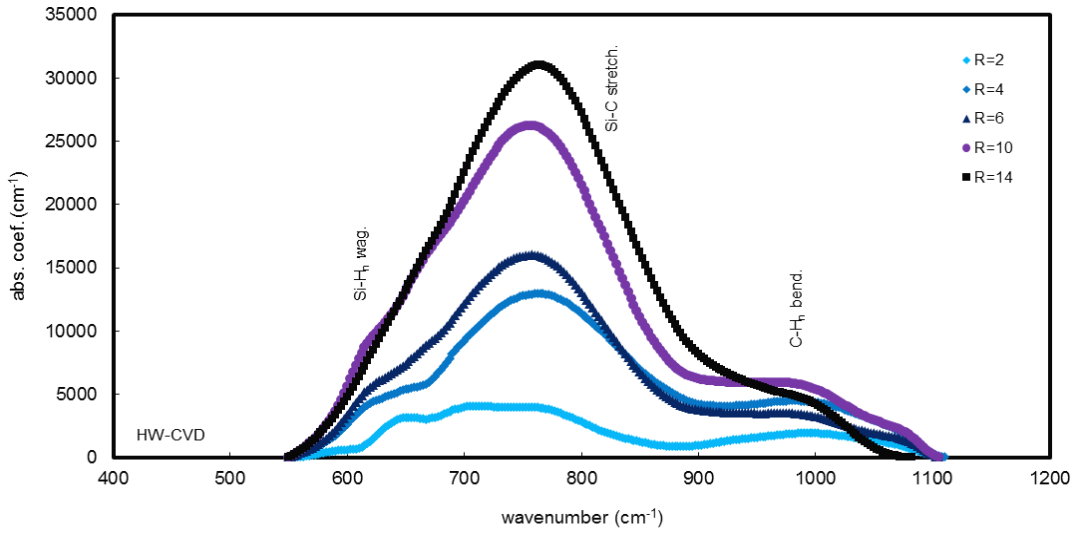

Figure 4.5(c): Absorption coefficient of vibration modes in 500-1500 cm^{-1} wavenumber region of SiC thin films prepared at different methane to silane gas flow rate ratio by HW-CVD technique.

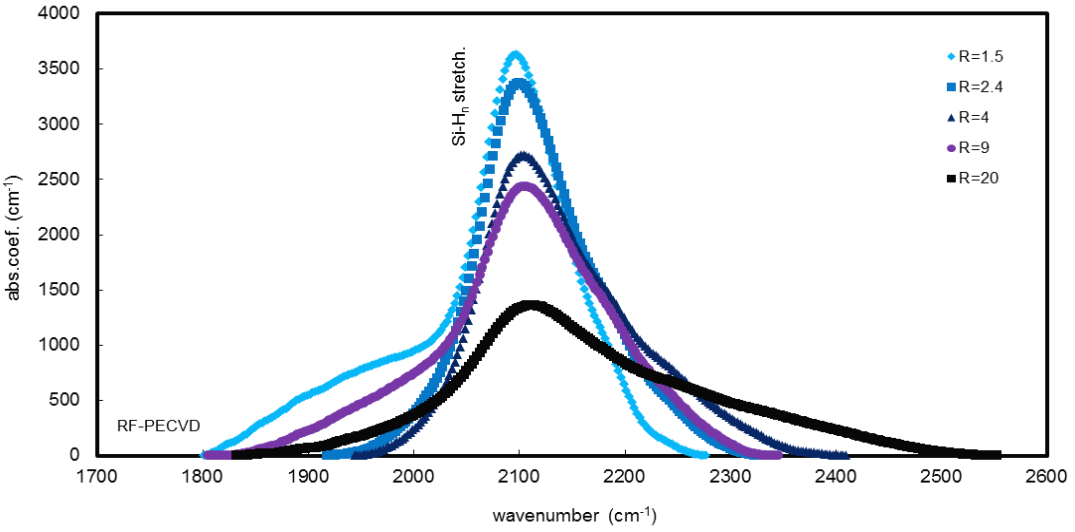

Figure 4.6(a): Absorption coefficient of Si-H_n stretching mode at approximately 2050 cm^{-1} of SiC thin films prepared at different methane to silane gas flow rate ratio by RF-PECVD technique.

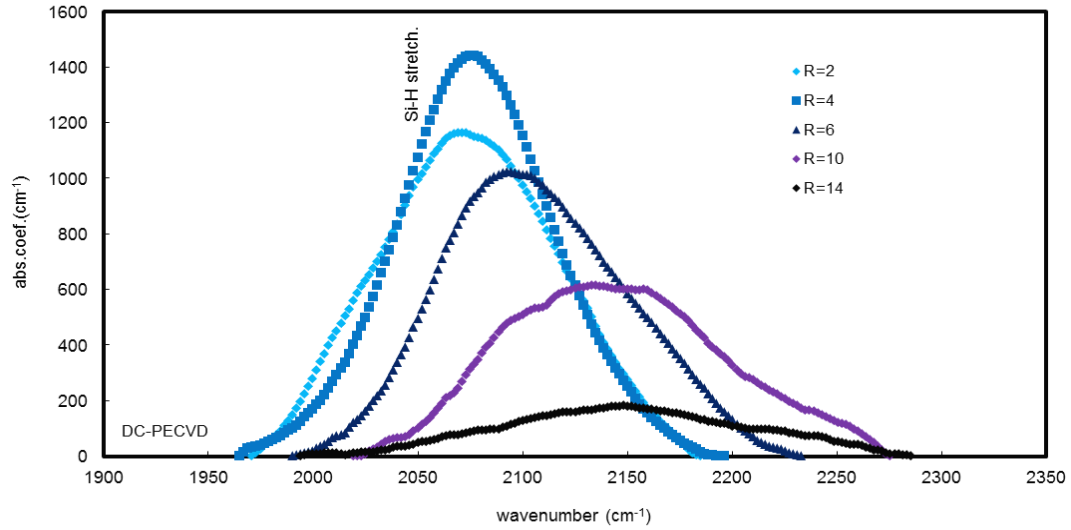

Figure 4.6(b): Absorption coefficient of Si-H_n stretching mode at approximately 2050 cm^{-1} of SiC thin films prepared at different methane to silane gas flow rate ratio by DC-PECVD technique.

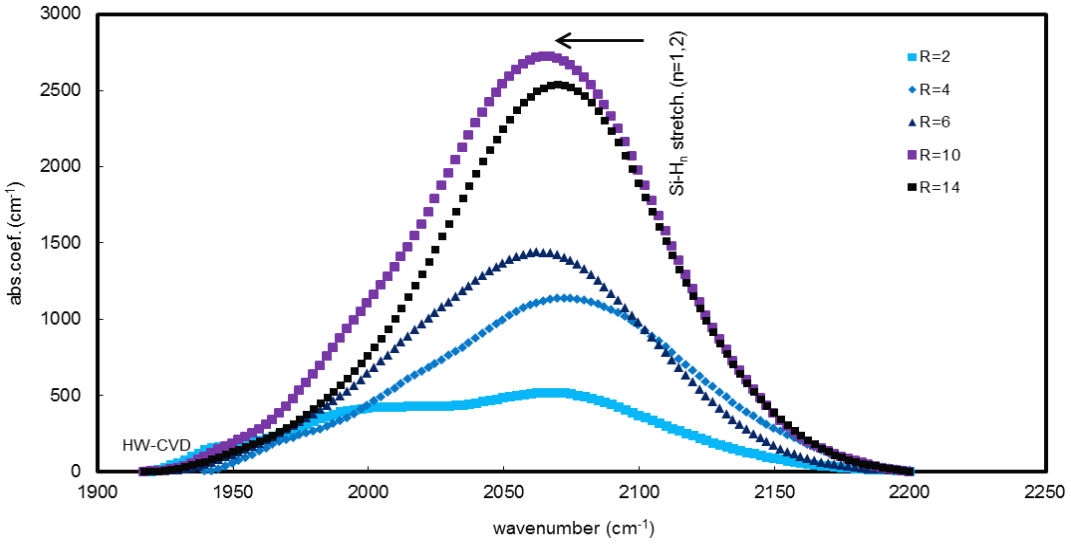

Figure 4.6(c): Absorption coefficient of Si-H_n stretching mode at approximately 2050 cm^{-1} of SiC thin films prepared at different methane to silane gas flow rate ratio by HW-CVD technique.

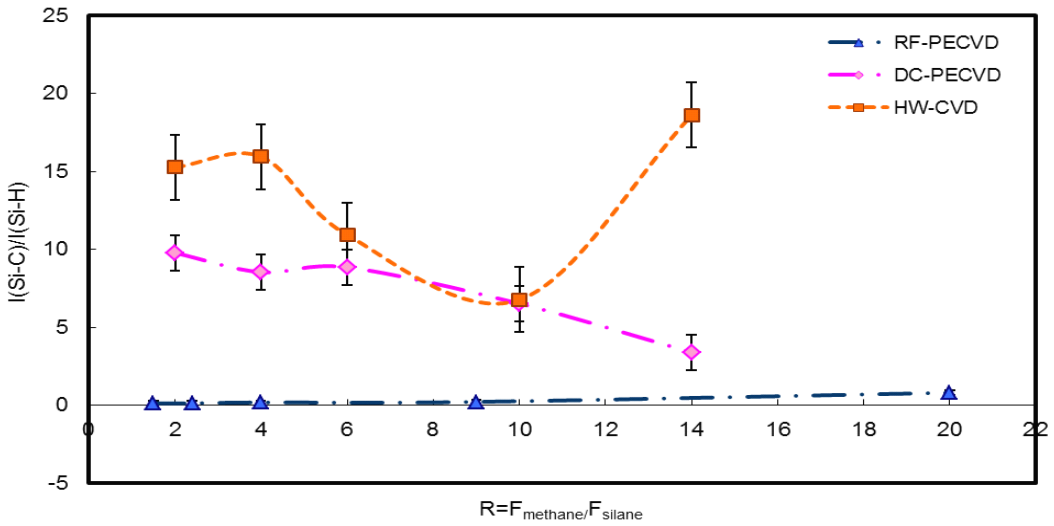

Figure 4.7: Integrated intensity of Si-C bands as compared to the Si-H_n bands for the SiC films prepared by RF-PECVD, DC-PECVD and HW-CVD techniques as a function of methane to silane gas flow rate ratio.

Figure 4.7 shows the variation of Si-C/Si-H to *R*. The results show that HW-CVD is more effective in a dominant Si-C phase in the CVD films in the range of *R* used in this work. Both RF-PECVD and DC-PECVD films were seen to have high a-Si:H phase compared to SiC phase. Increasing *R* reduces the SiC phase further. A slight increase in SiC phase are observed in the DC-PECVD film at the highest *R*. Table 2.3 in Chapter 2 shows the bonding energies of the bonds involved in the silicon carbide films studied in this work. Referring to Table 2.3, the bonding energy of Si-Si is the lowest followed by Si-H, Si-C, C-C and C-H in ascending order. Therefore at the silicon growth sites, diffusion of silicon atom is most favorable followed by hydrogen and carbon. At carbon growth sites however, bonding with silicon requires less energy than bonding with another carbon or hydrogen atom. Therefore, a hydrogen atom would have higher probability of bonding with silicon rather than carbon atoms. A silicon growth radical would have higher probability of bonding with silicon dangling bond rather than carbon dangling bond. A carbon dangling bond would have higher probability of bonding with silicon growth radical compared to hydrogen atom. At low

R, the pumping rate of the chamber is reduced to maintain the deposition pressure. Therefore, the energy of the growth radical reaching the growth surface is high and the probability of collision with methane molecule is low. The energetic growth radicals are able to create growth sites through abstraction process by breaking Si-H or C-H bonds followed by diffusion of these growth radicals onto these growth sites forming Si-C bonds. The low hydrogen atom concentration at the growth sites resulted in low concentration of Si-H or C-H bonds being formed. The hydrogen reaching the growth surface mainly etches weak bonds creating growth sites for more diffusion of growth radicals forming more Si-Si or Si-C bonds. The probability of diffusion of silicon atoms onto silicon dangling bond is higher than carbon atoms but the probability of forming C-C is very low as the diffusion energy is higher.

These factors increase the concentration of Si-C bonds in the films at low *R*. For DC-PECVD process, the Si-C/Si-H ratio remained high for films deposited up to *R* equals to 6 but decreased with further increase in *R*. The increase in hydrogen atoms at the growth sites increases the number of silicon and carbon dangling bonds but more silicon dangling bonds are expected to be formed since hydrogen etching effects has higher probability of breaking Si-Si bonds compared to C-C bonds or Si-C bonds due to their higher binding energy. The more dominant presence of hydrogen atoms at the growth sites and the concentration of these hydrogen atoms are expected to be lower due to increased collision with methane molecules at high *R*. Therefore, the probability for the formation of Si-H bonds would be higher as compared to Si-C bonds. As for the HW-CVD process, the Si-C/Si-H ratio decreases at a lower *R* value of 4 compared to the DC-PECVD films for similar reason.

The Si-C bond are higher for the films prepared at *R* equal to 2, 4 and 6 compared to DC-PECVD films since dissociation of methane molecules is more

reactive by DC-PECVD. The increase in Si-C/Si-H ratio for the HW-CVD films prepared at the highest *R* of 14 is due to depletion of hydrogen atoms as a result of increase in secondary gas phase reaction with methane molecules. This does not happen for the DC-PECVD process since the rate of methane dissociation is significantly higher compared to HW-CVD process. The significantly lower Si-C/Si-H ratio is for the film prepared by DC-PECVD process and is due to the low dissociation rate of the silane and methane molecules as the power is very low compared to DC-PECVD process. The slight increase in the ratio of at the highest *R* is also due to depletion of hydrogen atoms with increase in secondary gas phase reaction with methane molecules.

4.4 X-Ray Diffraction Spectra of Silicon Carbide Thin Films Prepared at Different Methane to Silane Gas Flow Rate Ratio

The XRD spectra for the silicon carbide films prepared by RF-PECVD, DC-PECVD and HW-CVD techniques at various *R* value is shown in Figure 4.8(a), Figure 4.8(b) and Figure 4.8(c) respectively.

Evidence of crystalline structure is not observed in the XRD spectra for all the silicon carbide films prepared by RF-PECVD. All the spectra showed a broad diffraction peak in the range of 15^o to 40^o with the peak centered approximately at $2\theta = 28.5^o$. Swain (Swain *et al.,* 2006) contributed this broad peak to lack of long range order in the film structure.

The XRD spectra for the silicon carbide films prepared by DC-PECVD technique at various *R*, is shown in Figure 4.8(b). The silicon carbide films show a rather broad diffraction peak at $2\theta = 57^o$ which could be due to the existence of face-centered cubic-Si crystals (Tabata and Komura, 2007, Wang *et al.,* 2007). For their preparation of nanocrystalline cubic SiC thin films, they assigned diffraction peaks at $2\theta=60.0^o$ and $2\theta=71.7^o$ to (220) and (311) oriented crystallites of 3C-SiC respectively

but silicon carbide films prepared in this work do not show any existence of those. This indicates that the crystallite structures in the silicon carbide films prepared by DC-PECVD in this work are Si-cystals. The peak intensity increases and the FWHM of the peak decreases for the film prepared at highest *R* of 14. The absence of any evidence of SiC crystal structure suggests that the Si-C bonds are of short range order thus the film is mainly amorphous silicon carbide with cubic Si-crystals embedded within it.

Silicon carbide films prepared by HW-CVD technique at various *R* value produced XRD spectra similar to the films prepared by DC-PECVD as could be seen in Figure 4.8(c). The silicon carbide films prepared by HW-CVD also show diffraction peaks at $2\theta=57^{o}$ which show the existence of face-centered cubic-Si crystals. However, the signal for this diffraction signal is only clear for films prepared at low methane to silane gas flow rate ratio (R=2, R=4, and R=6) but is very weak for silicon carbide films prepared at high methane to silane gas flow rate ratio (R=10 and R=14). This result indicates that silicon carbide films prepared by HW-CVD consist of cubic-Si crystals when methane to silane gas flow rate ratio is relatively small. Similar to the silicon carbide films prepared by DC-PECVD technique, the Si-C bonds are of short range order thus the film is mainly amorphous silicon carbide with cubic Si-crystals embedded within it. For silicon carbide films prepared at high methane to silane gas flow rate ratio (R=10 and R=14), the film structure is totally amorphous. This is also true for the silicon carbide film prepared with R=14 where the Si-C/Si-H intensity ratio is high.

Generally, increase in *R* would result in increase in hydrogen and carbon radicals. This enhanced hydrogen treatment affects creating growth sites. Since the diffusion energy of silicon atoms on to the silicon growth sites is lower, probability of forming Si-Si bonds are higher. The higher presence of hydrogen radicals enhances

etching effects thus increasing the structural order. This induces the formation of silicon nanocrystallites.

The dissociation of methane molecules by DC-PECVD produced more hydrogen atoms compared to the dissociation of this gas by the hot-wire tungsten filament. It is suggested (Duan *et al.,* 2001) that methane decomposed to CH_3 and CH radicals in HW-CVD process. However in this work, methane molecule is hardly decomposed by the 1700°C filament temperature. Therefore at high *R*, it is suggested that with the high amount of hydrogen radicals from decomposition of silane, energy transferred by collisions with the increased number of methane molecules has enabled diffusion of carbon into Si dangling bonds thus increasing the Si-C/Si-H intensity ratio (Figure 4.7). With these effects also it is found that the film is more amorphous in structure.

In their study on the structure of silicon carbide films doped with Cobalt, Sha *et al.* (2006) assigned a peak at $2\theta=33.6^{o}$ to SiC(101). For all the silicon carbide films prepared in this work, this sign is unavailable.

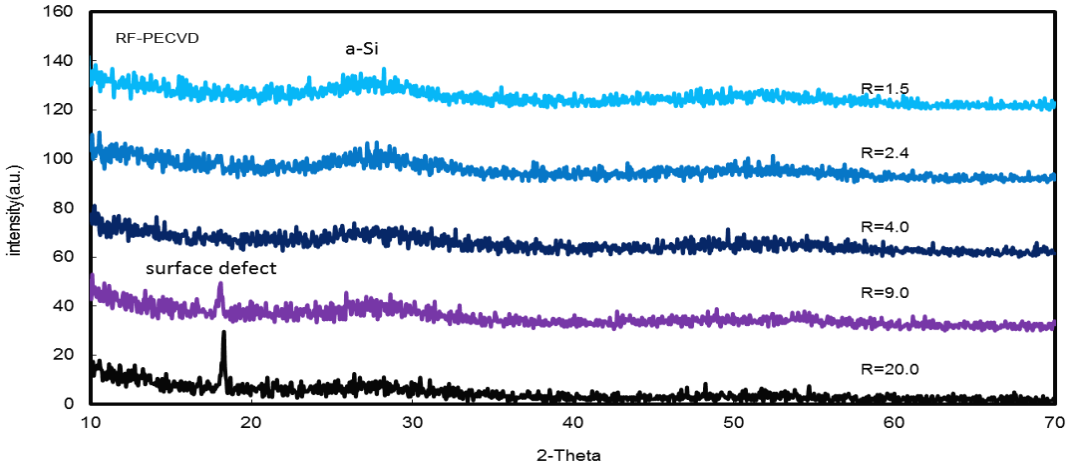

Figure 4.8(a): XRD spectra of SiC thin films prepared at different methane to silane gas flow rate ratio by RF-PECVD technique.

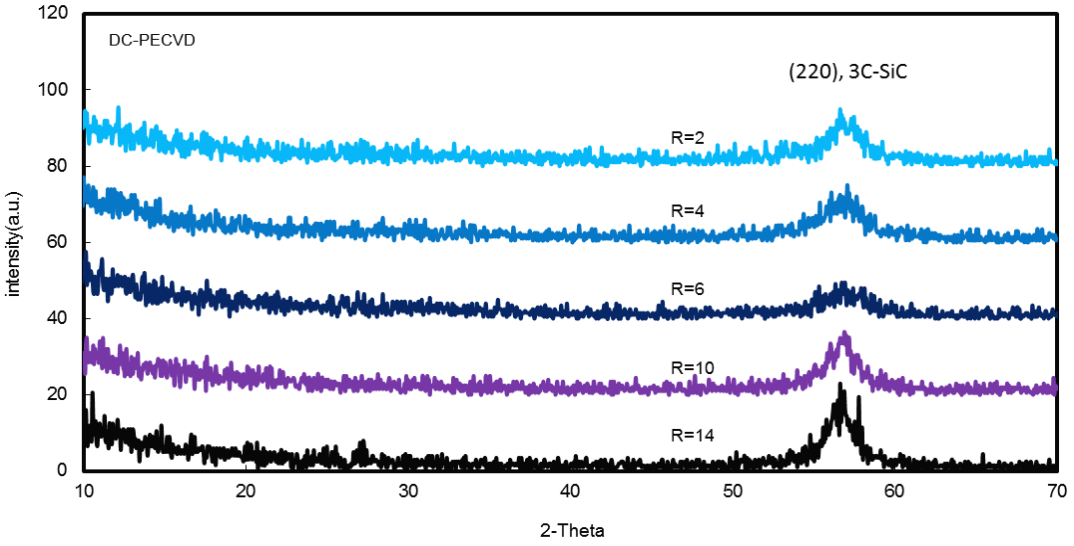

Figure 4.8(b): XRD spectra of SiC thin films prepared at different methane to silane gas flow rate ratio by DC-PECVD technique.

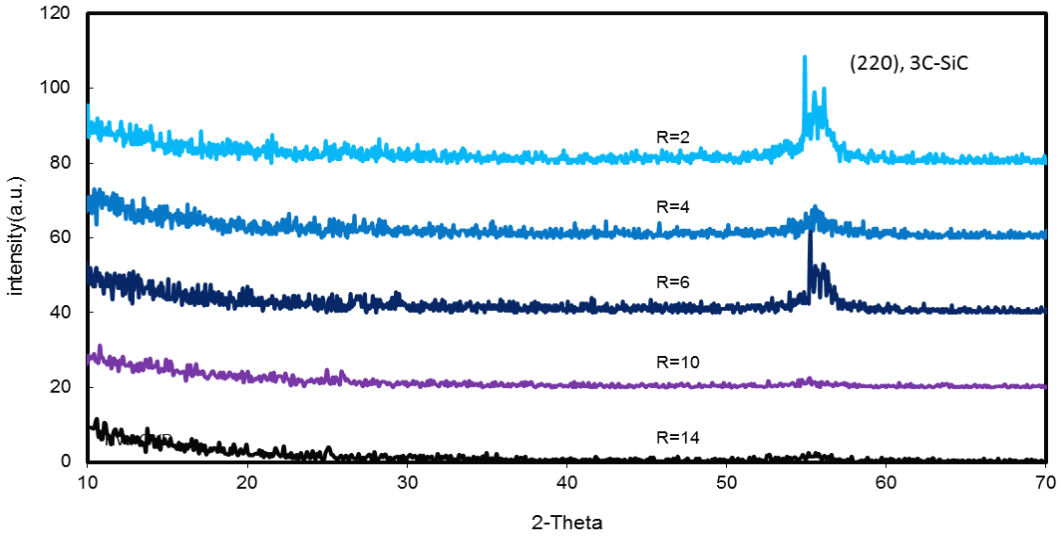

Figure 4.8(c): XRD spectra of SiC thin films prepared at different methane to silane gas flow rate ratio by HW-CVD technique.

4.5 Micro-Raman Spectra of Silicon Carbide Thin Films Prepared by RF-PECVD, DC-PECVD and HW-CVD Techniques at Different Methane to Silane Gas Flow Rate Ratio

Micro-Raman spectra for the silicon carbide films prepared by RF-PECVD, DC-PECVD and HW-CVD techniques is shown in Figure 4.9(a), Figure 4.9(b) and Figure 4.9(c) respectively.

Figure 4.9(a) shows the Micro-Raman spectra for silicon carbide thin films prepared by RF-PECVD at various *R*. Amorphous Si-Si (Transverse Optical) mode at 475-480 cm^{-1} (Xu *et al.,* 2003, Xu *et al.,* 2005, Swain and Dusane, 2006) is observed for all samples but the n-Si vibrational mode at 500 cm^{-1} is only present for the sample prepared at the highest *R* (*R*=20). The peaks corresponding to the longitudinal (790 cm^{-1}) and transverse optical (970 cm^{-1}) phonons of SiC (Yu *et al.,* 2000, Wieligor *et al.,* 2005, Klein *et al.,* 2006) is not detected in any of the samples prepared at low *R* but a broad peak is identified for these peaks for samples prepared at high *R* (*R*=9, 20). Some weak bands in the region between 600 and 1000 cm^{-1} may have resulted from low Raman efficiencies of the Si-C bands (Swain and Dusane, 2006).

Consistent with the XRD results, the micro-Raman spectra for RF-PECVD films were all amorphous producing a broad amorphous peak at around 480 cm^{-1}. A broad peak observed in the region of 960 cm^{-1} for silicon carbide films prepared at large *R* showed that silicon carbide nanocrystallites were present. The broad peak indicated that these nanocrystallites were very small. Referring to Figure 4.8(a), XRD peak due to SiC nanocrystals at $2\theta = 28.5^{o}$ might have been buried by the broad amorphous peak in this region. The higher concentration of hydrogen radicals reaching the substrate due to increase in concentration of methane molecules at high *R* incorporated carbon atoms into the film structure in the form of small silicon carbide nanocrystalline structures. However, the abundant amount of hydrogen radicals has higher probability of diffusing onto silicon dangling bonds as the diffusion energy is lower compared to carbon radicals. This resulted in the formation of very small SiC nanocrystallites surrounded by a dominant region of hydrogenated amorphous silicon (a-Si:H) matrix.

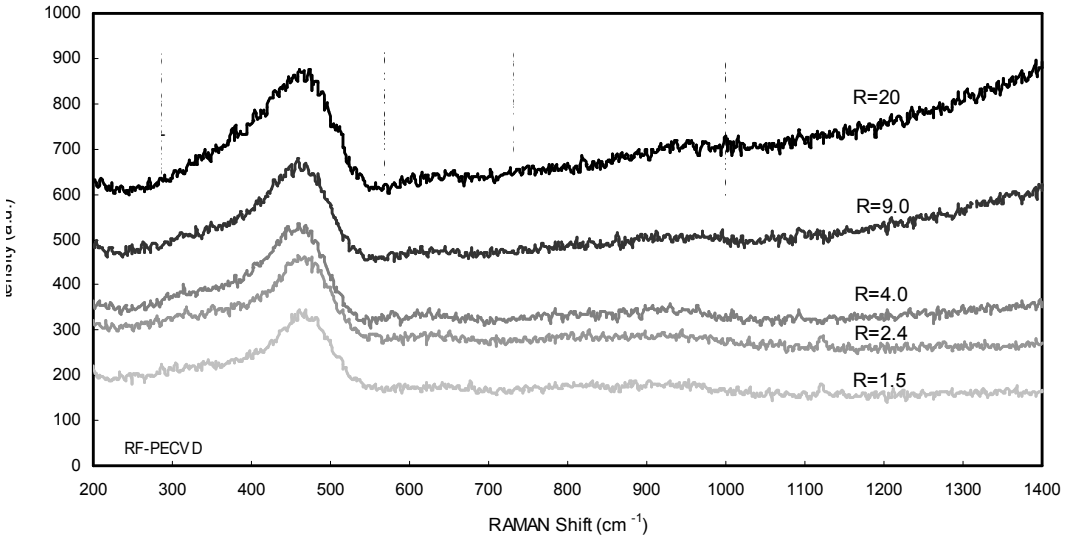

Figure 4.9(a): Micro-Raman spectra of SiC thin films prepared at different methane to silane gas flow rate ratio by RF-PECVD technique.

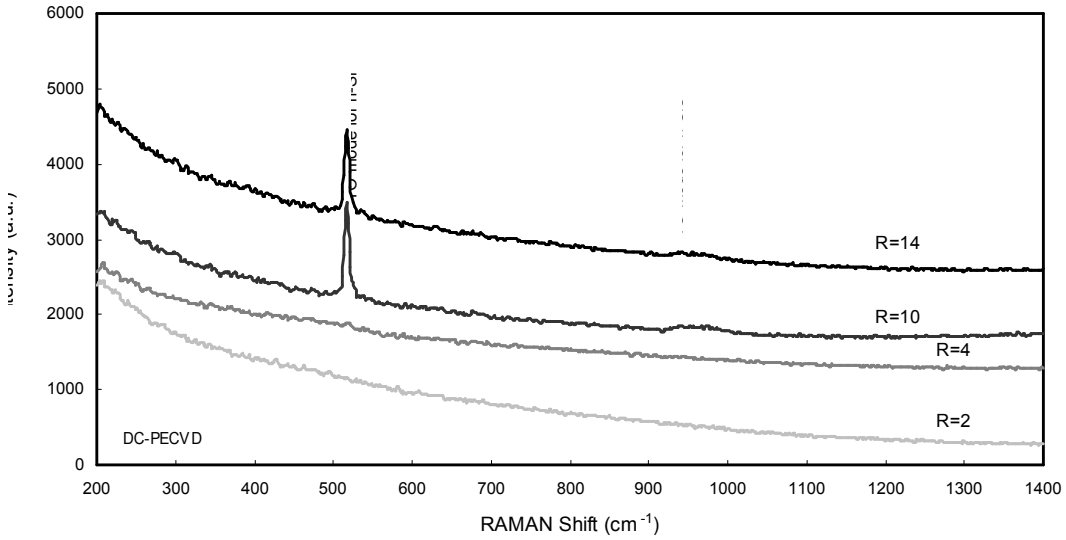

Figure 4.9(b): Micro-Raman spectra of SiC thin films prepared at different methane to silane gas flow rate ratio by DC-PECVD technique.

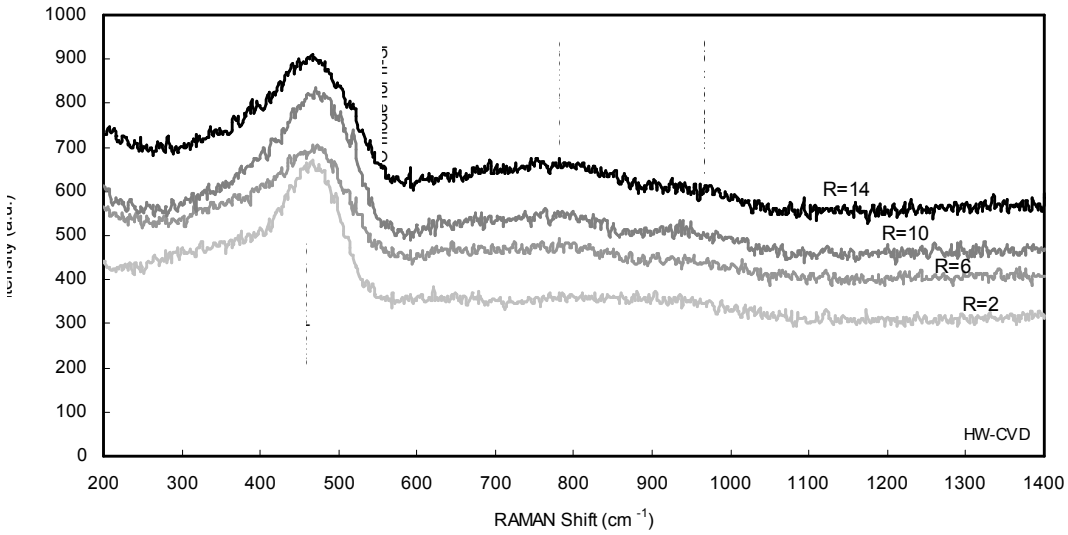

Figure 4.9(c): Micro-Raman spectra of SiC thin films prepared at different methane to silane gas flow rate ratio by HW-CVD technique.

Figure 4.9(b) shows the Micro-Raman spectra for silicon carbide films prepared by DC-PECVD technique at various *R*. There is no significant peak obtained for these films prepared at low *R* (*R*=2,4) indicating that they are mainly amorphous. Otherwise, silicon carbide films prepared at higher *R* (*R*=10,14) show obvious crystalline-Si peak at 517 cm^{-1} (King *et al.,* 2011). Xu (Xu *et al.,* 2003) attributed this peak to TO mode of Si nanocrystals and any vibration band at 500 cm^{-1} to the vibration mode related to the interfaces of Si nanocrystals with a-Si matrix (Song *et al.,* 2011).

In this figure (4.9(b)), the presence of a sharp peak at around 520 cm^{-1} for the films prepared at high *R* of 10 and 14 indicates the presence of silicon nanocrystallites in the film structure. The intensity of the peak is lower for the film prepared at higher *R* (*R*=14) as compared to the film prepared at *R*=10. The presence of the sharp Raman peak at 520 cm^{-1} strongly suggested that this broad peak was due to the second order Raman band of silicon (Song *et al.,* (2011). Therefore the results strongly indicated that the silicon nanocrystallites were embedded in silicon carbide amorphous phase.

The broad band observed at 960 cm^{-1} is usually associated with crystalline SiC presence but this band also co-exists with the second order Raman band of crystalline

silicon at 970 cm^{-1}. In this work, it is also observed for these films (R=10,14) that a weak broad peak exists between 900 cm^{-1} and 1000 cm^{-1} which is suspected to be the signature of transverse optical (TO) phonons of crystalline SiC as reported by Yu (Yu *et al.,* 2000). This results conforms the results depicted from the XRD spectra that silicon carbide films prepared by DC-PECVD in this work consists of Si crystalline structures embedded within amorphous Si-C matrix. At high methane to silane gas flow rate ratio also, traces of crystalline Si-C is observed.

The Micro-Raman spectra for silicon carbide films deposited by HW-CVD at various R can be observed in Figure 4.9(c). The spectra are similar to the spectra obtained for the silicon carbide films prepared by RF-PECVD. All the films present a broad peak at 300-500 cm^{-1} and centered at 480 cm^{-1} which is attributed to Si-Si phonons (Ricciardi *et al.,* 2006). This result shows that the presence of short range order Si-Si bond is very dominant in the film. This is depicted from the amorphous Si-Si (Transverse Optical) mode at 475-480 cm^{-1} (Xu *et al.,* 2003, Xu *et al.,* 2005, Swain and Dusane, 2006, Yu *et al.,* 2004) which is observed for all films. The spectra suggest that the amorphous-Si phase is dominant in this film and the film is Si-rich (Yu *et al.,* 2004). Itoh *et al.* (2001) reported that they obtained a-SiC:H films with embedded Si-nanocrystallite by HW-CVD using CH_4 as a carbon source. In this work where silicon carbide films is prepared by HW-CVD, appearance of a broad peak at 600-1000 cm^{-1} was observed as the silicon carbide films were prepared with higher values of R. It consists of several vibration bands such as 620 cm^{-1}, 790 cm^{-1} and 960 cm^{-1} which corresponds to $Si\text{-}H_n$ wagging and the second order LA mode of Si-Si vibration, Si-C vibration mode and the second order TO mode of Si-Si vibration respectively (Yu *et al.,* 2004). This result shows that silicon carbide films deposited using HW-CVD is mainly built of mixture of amorphous-Si and amorphous SiC with crystalline-Si structures

embedded within it. This agrees with the discussion from the XRD results in sub-section 4.4 that the films prepared at lower methane to silane gas flow rate ratio (R=2,4,6) are mainly amorphous in structure with traces of cubic Si-crystals and the films prepared at higher ratio (R=10,14) are totally amorphous.

In order to facilitate the discussion on the morphology of the prepared thin films, AFM microscopic study were done on several samples. The images and its roughness analysis were presented in Appendix C. Compatibility of the columnar structures that were seen in the AFM images to the crystalline peaks discussed in the previous sub-sections has led to the believe that they are representative of each other. Otherwise, where the grain size were uniform (Wang *et al.,* 2007) and mean roughness were relatively low, the film would show amorphous on the XRD and Micro-Raman spectra.

4.6 Summary

The home-built PECVD system comprising of RF-PECVD, DC-PECVD and HW-CVD techniques had successfully been used to prepare silicon carbide thin films. This work has showed that each deposition technique built in the system can be utilized individually to produce silicon carbide thin films with various film properties. It was found that by applying a variable range of methane to silane gas flow rate ratio, the film deposition rate and optical energy band gap could be divert in different manners for different techniques. RF-PECVD technique from the system could produce silicon-rich amorphous silicon carbide thin films with deliberately high optical energy band gap. DC-PECVD technique displayed low deposition rate as compared to the other techniques but produces silicon carbide thin films with relatively high optical energy band gap with traces of silicon nanocrystallites embedded in its amorphous structure. On the other hand, silicon carbide thin films prepared by HW-CVD technique exhibit

promising properties such as high deposition rate, increasing value of optical energy band gap and displaying short-range ordered structure with increased methane to silane gas flow rate ratio. The hybrid HW-PECVD system discussed in the next chapter follows the parameters that were utilized in this section with the methane to silane gas flow rate ratio was fixed to the highest and lowest value (R=14 and R=2).